

PS15

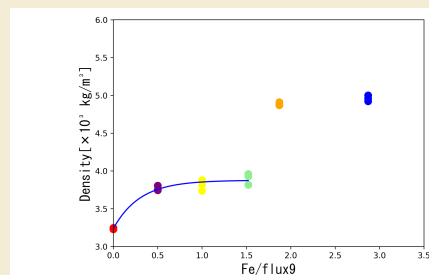
溶融Feと酸化物融体による複合液滴の体積変化

Volume change of compound droplet by liquid Fe and molten oxides by mass transfer through interface under microgravity

松本彩里^{1,*}, 佐藤令奈¹, 渡邊匡人², 松下泰志³, 小山千尋⁴Irori MATSUMOTO^{1,*}, Reina SATO¹, Masahito WATANABE², Taishi MATSUSHITA³ and Chihiro KOYAMA⁴¹ 学習院大学自然科学研究科, Graduate School of Science, Gakushuin University, Tokyo, Japan² 学習院大学理学部, Faculty of Science, Gakushuin University, Tokyo, Japan³ Department of Materials and Manufacturing, Jönköping University, Jönköping, Sweden⁴ Japan Aerospace Exploration Agency, JAXA, Tsukuba, Japan

* Correspondence: 24141009@gakushuin.ac.jp

Abstract: Interfacial phenomena occur when two immiscible liquids come into contact with each other and are of interest in a variety of scientific and technical fields. Understanding and observing the interfacial phenomena between molten oxide and liquid iron (Fe) is of great importance in controlling the steelmaking process. We are studying the interfacial phenomena by observing composite droplets composed of molten oxide and liquid iron in the electrostatic levitation furnace (ELF) of the International Space Station (ISS). Since there is no density difference in the microgravity environment, the composite droplets form core-shell droplets. While observing melting at a constant temperature, we observed the increase in liquid volume. This volume expansion was attributed to the dissolution of Fe from the core liquid to the shell melt oxide at the interface due to the oxidation of liquid Fe. To clarify this hypothesis, it is necessary to investigate the volume change of the core-shell droplet. Therefore, we measured the density of the molten oxide when Fe was dissolved into the molten oxide using the aerodynamic levitation method on the ground and analyzed the volume change. Through these analyses, the oxidation of liquid Fe at the interface with the molten oxide was discussed.



Keywords: International Space Station, Electrostatic Levitation Furnace, Microgravity, Compound Droplet, Density of High Temperature Liquid

1. Introduction

Interfacial phenomena between immiscible liquids are intriguing in many fields from scientific and technological viewpoints. Liquid iron (Fe) and molten oxides are immiscible, and their immiscibility is used in the steel industries, including smelting, continuous casting, and welding. Understanding and observing the interfacial phenomena between molten oxide and liquid Fe is crucial for process control in steel manufacturing. During the separation process, liquid Fe is placed at the bottom due to its significant difference in density compared to molten oxide under normal ground conditions. Therefore, X-ray radiographs were used during ground experiments to observe the interface between molten oxides and liquid Fe by immersing a drop of liquid Fe in a molten oxide bath.¹⁾ During the observation using X-rays, the shape of the liquid Fe was clearly visible, but the changes in the molten oxide could not be detected from the slight contrast of the X-ray through the molten oxide parts.²⁾ Thus, previous studies of liquid Fe immersed in molten oxides, including the interface between them, did not consider the change in the molten oxides. However, when molten oxide and liquid Fe are combined under microgravity conditions, they form a core-shell droplet due to their interface and surface-free energies. For a compound drop of molten oxide and liquid Fe, the molten oxide forms a shell around the liquid Fe due to its lower surface tension.

We studied the interfacial phenomena by observing the surface oscillation of the core-shell droplets of molten oxide and liquid Fe in the electrostatic levitation furnace (ELF)^{3–6)} onboard the International Space Station (ISS). We formed a coreshell droplet by molten oxide ($\text{SiO}_2\text{:CaO:Mn}_3\text{O}_4\text{:TiO}_2\text{:Fe}_2\text{O}_3 = 25\text{:}7\text{:}20\text{:}18\text{:}30$ mass%) and liquid Fe in an Ar atmosphere. The molten oxide composition is designed for welding fluxes. The molten oxides used in welding flux have good wettability to the liquid Fe, enabling coverage of the liquid Fe parts. The molten oxides fully cover the liquid Fe droplet. Therefore, liquid Fe is prevented from contacting atmospheric Ar gas conditions. In these conditions, we observed an increase in core-shell droplet volume.⁷⁾ We also observed a reduction in the core Fe volume through X-ray radiography after the samples returned to Earth from the ISS.⁷⁾ This result might be due to the liquid Fe oxidation at the interface with the molten oxide. The phenomenon could not be observed previously in ground experiments using X-ray radiography for the system of a liquid Fe drop immersed in a molten oxide bath. Since the view area of the X-ray radiograph was close to the interface between the molten oxide and liquid Fe, the molten oxide volume could not be measured.²⁾

From the background, we analyzed the volume increase in the core-shell droplets by molten oxides and liquid Fe under the hypothesis that Fe dissolves into the molten oxide from the core liquid Fe by oxidizing liquid Fe at the interface to the molten oxides. If Fe dissolves into molten oxide, the density of the molten oxide will change. We must determine the density change of the molten oxide used as the shell for coreshell droplets with Fe additions to analyze the volume change. Therefore, we investigated in more detail the density changes of molten oxide by adding Fe using the aerodynamic levitation (ADL) method on the ground. These measurements allow us to discuss the oxidation of liquid Fe at the interface with the molten oxide.

2. Forming composite droplets using ELF in ISS

The core-shell droplet samples consisting of molten oxide and liquid Fe were prepared on the ground using a two step ADL method. First, spherical samples of Fe and oxide were prepared, then oxide samples were heated and melted using a CO_2 laser, and Fe spheres were dropped into the melt. The spherical Fe sample was incorporated into the oxide melt by the action of interfacial tension, and then quenched to obtain a solid composite droplet with a radius of about 2 mm. The oxide sample used was a model composition of flux material used in the welding process ($\text{SiO}_2\text{:CaO:Mn}_3\text{O}_4\text{:TiO}_2\text{:Fe}_2\text{O}_3 = 25\text{:}7\text{:}20\text{:}18\text{:}30$ mass%, Flux-9 for our named). Fe samples were prepared using the electro-refining method to reduce the oxygen concentration.

In the ELF installed on the ISS, four semiconductor lasers with a 980 nm wavelength were used to heat and melt the solid composite, forming a core-shell droplet. The sample was kept at a constant temperature at the center of the ELF electrodes. The atmospheric conditions in the ELF during sample melting were Ar gas atmosphere at 0.2 MPa. The shape of the sample as it was melting was observed using a standard-speed charge-coupled device camera at 60 fps, and the formation of core-shell droplets showed a perfect circular shadow. When observing the shape of the molten sample, the volume of the entire core-shell droplet was also simultaneously obtained from its shape using backlight optics. The sample temperature was measured as an apparent temperature using a single-color pyrometer with a wavelength range of 1.45–1.8 μm and an emissivity set to 1.0. This apparent temperature was corrected using the emissivity of the sample and the system constants, as described in.⁸⁾ The emissivity of the Flux-9 oxide is 0.76, a value obtained by our own method based on the melting point of liquid Fe and its emissivity.⁹⁾

3. Volume change of core-shell droplets composed of liquid Fe and molten oxides

The sample was generally spherical during melting, but the sphere was partially deformed in were deformed in the early stages of heating. This is thought to be due to changes in the total free energy due to surface and interfacial tension and its area. After a few minutes, the sample became spherical again due to the change in interfacial area. The volume of the core-shell droplet was measured from the sample geometry during melting, and it was found that the volume increased linearly with time under constant temperature (**Fig.1**). This trend was confirmed for all composite samples tested at ELF, with the example in **Fig.1** held at 1610 °C for 1.2×10^3 s. The core-shell sample volume is V_{total} , and the initial volume is V_{total}^0 , as shown in **Fig.1**. X-ray results before and after the experiment (**Fig.2**) show that the volume of core Fe decreased while the mass of the entire droplet remained unchanged. After solidification, the Fe in the core was distorted rather than spherical, which may be due to differences in volume shrinkage of Fe/Flux-9 and other factors. As shown in **Fig.3**, the distorted core shape was approximated by two circles and the volumes were calculated as spherical base and spherical lack. Using the density of solid Fe to determine the mass^{10),11)}, the mass of core Fe decreased from 12 mg to 9.88 mg.

From this, it is concluded that the increase in volume is the result of core Fe being oxidized and dissolved into the shell oxide. It can be assumed that the volume of Fe incorporated into the shell oxide is proportional to the amount of dissolved Fe. To accurately determine the volume in the molten state, the density and mass of the Fe-containing oxide are required. Since the reduced mass of Fe is available from the X-ray results and the mass

of the entire sample remains the same, we can assume that all of the reduced mass has been dissolved into the shell. Under this assumption, we investigated the density variation of Flux-9 oxides with Fe content using a combination of ELF and ADL on the ground.^{12),13)}

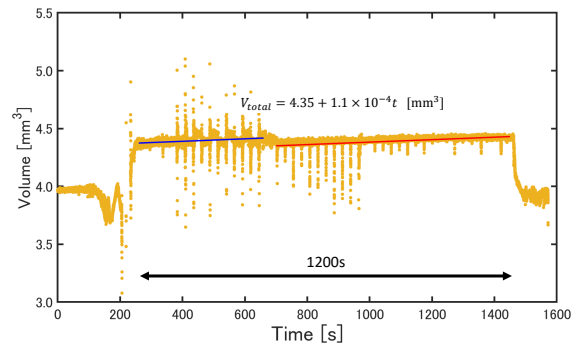


Figure 1. Volume change of the core-shell droplet with time at 1610 °C; the significant deviation is originated from the sample position change by applying as electrical field to excite the drop oscillations.

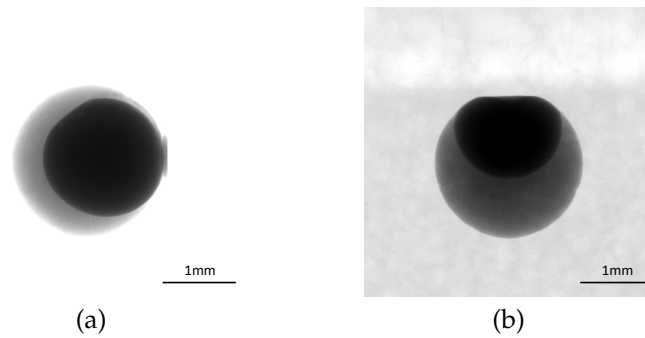


Figure 2. X-ray radiograph images of solidified core-shell drop samples after being processed by the electrostatic levitation furnace (ELF) in the International Space Station (ISS):(a) Observation image from a direction parallel to main electric field directions and (b) observation image from a direction perpendicular to the main electric field directions.

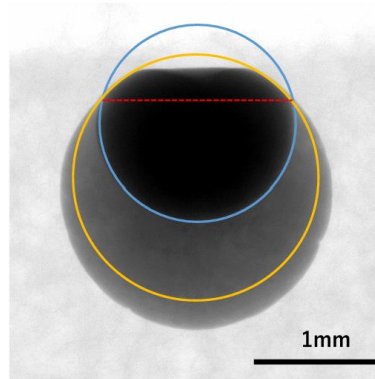


Figure 3. The core Fe volume determination method using the fitting of core Fe parts by two circles. The radii of fitted circles were used to approximate the upper region delineated by the red dashed line as a spherical cap and the lower part as a spherical segment. The volumes of these regions were calculated individually and summed to obtain the total volume of the core Fe.

4. Density changes of molten oxides of Flux-9

The density of Flux-9 without Fe was measured under microgravity using the ELF, under the same conditions as the core-shell droplet experiments. The measurement method is described in detail elsewhere.³⁾ For temperature correction, we applied the same procedure as in the core-shell experiments using the emissivity value of 0.76 for Flux-9 molten oxides, previously determined by our group.⁹⁾ As a result, the density at the liquidus temperature was found to be $3.27 \times 10^3 \text{ kg/m}^3$, in good agreement with the calculated value of $3.24 \times 10^3 \text{ kg/m}^3$ obtained using ThermoCalc 2023a with the TCOX12 database.¹⁶⁾ Therefore, the calculated value was used as the representative density of Flux-9 at the liquidus temperature.^{12),13)} In contrast, due to

limitations in sample preparation before launch, it was not possible to measure the density of Fe-containing Flux-9 oxides using the ELF. Instead, we conducted density measurements of Flux-9 with added Fe using the ADL on the ground. Samples were prepared by mixing oxide powders with electro-refined Fe powder, followed by milling and CO₂ laser sintering into spherical shapes. Measurements were performed in an open system, with the sample floated by Ar gas and the chamber open. In ADL, the lower part of the sample is hidden by the nozzle, and aerodynamic and gravitational effects distort the shape from a perfect sphere. Therefore, the uncertainty of measurement (UOM) is larger $\pm 10\%$ than in ELF. Nevertheless, the results from ELF and ADL showed consistency, allowing evaluation of density changes as a function of Fe content.⁷⁾ As the Fe mass ratio ($x = m_{\text{Fe}}/m_{\text{ox}}$) increased, the density of the molten oxide rose initially and then plateaued above $x = 1.9$ (Fig.4). In this range, the density increased from 3.24×10^3 to $3.75 \times 10^3 \text{ kg/m}^3$, consistent with the predicted value at equilibrium with liquid Fe from ThermoCalc ($3.49 \times 10^3 \text{ kg/m}^3$). The density change with Fe content was fitted by the following equation:

$$\rho_{\text{ox+Fe}} = 0.6403(1 - e^{-3.3374x}) + 3.24[\times 10^3 \text{ kg/m}^3]. \quad (1)$$

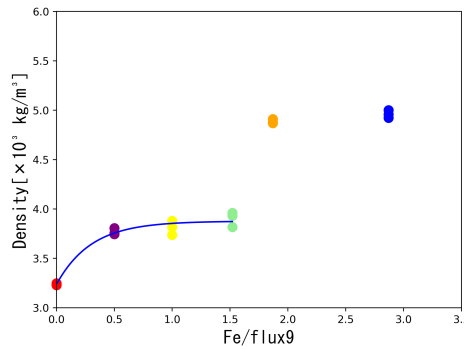


Figure 4. The density of Fe-added Flux-9 oxides was measured on the ADL method. The mass ratio between Flux-9 and Fe was varied for each sample, and the corresponding density values were obtained. The results indicate that the density of the molten oxide increases with Fe addition and becomes saturated when the Flux-9 to Fe mass ratio exceeds 1.9. A fitting curve was applied to the density data up to Fe mass ratio of 1.5, yielding an empirical expression for the density variation as a function of Fe content.

5. Investigation of shell oxide volume expansion induced by core Fe dissolution

Since the experimental samples were composed of Fe and oxides, the total volume of the sample can be expressed as the sum of the Fe core volume (V_{Fe}) and the shell oxide volume (V_{shell}).

$$V_{\text{total}} = V_{\text{Fe}} + V_{\text{shell}} \quad (2)$$

As described above, X-ray radiographic observations confirmed a reduction in the core Fe volume. Given that the total mass of the sample remained unchanged before and after the experiment, it is considered that the core Fe dissolved into the surrounding oxide shell. Using the reduced Fe mass (Δm_{Fe}), the mass of core Fe and oxide can be expressed as follows, where m^0 denotes the initial mass:

$$m_{\text{Fe}} = m_{\text{Fe}}^0 - \Delta m_{\text{Fe}}, \quad (3)$$

$$m_{\text{ox}} = m_{\text{ox}}^0 + \Delta m_{\text{Fe}}. \quad (4)$$

Additionally, by applying the definitions of density as the ratio of mass to volume for both Fe ($m_{\text{Fe}}/V_{\text{Fe}}$) and oxide ($m_{\text{ox}}/V_{\text{ox}}$), the reduced Fe mass can be as shown in Eq.(5). Using this, the total initial mass of the compound droplet is given by Eq.(6).

$$\Delta m_{\text{Fe}} = m_{\text{Fe}}^0 - \rho_{\text{Fe}} V_{\text{Fe}}, \quad (5)$$

$$m_{\text{Fe}}^0 + m_{\text{ox}}^0 = \rho_{\text{Fe}} V_{\text{Fe}} + \rho_{\text{ox}} V_{\text{ox}}. \quad (6)$$

Given the dissolution of core Fe into the surrounding oxide shell, the density of the oxide in Eq.(5) can be described using the density variation value with respect to Fe content given in Eq.(1).

$$m_{\text{Fe}}^0 + m_{\text{ox}}^0 = \rho_{\text{Fe}} V_{\text{Fe}} + \rho_{\text{ox+Fe}} V_{\text{ox}} \quad (7)$$

The liquid Fe density ρ_{Fe} is used the reported data of Refs^{14,15}. From Eq.(2) and Eq.(7), the volumes of the oxide shell (V_{shell}) and the core Fe (V_{Fe}) can be expressed in terms of the total volume, densities, and the initial masses of the oxide and core Fe, thereby quantifying the volume changes in the composite droplet. The total volume of the sample (V_{total}) and the density of the oxide ($\rho_{\text{ox+Fe}}$) change over time.

$$V_{\text{shell}} = \frac{\rho_{\text{Fe}}}{\rho_{\text{Fe}} - \rho_{\text{ox+Fe}}} V_{\text{total}} - \frac{m_{\text{ox}}^0}{\rho_{\text{Fe}} - \rho_{\text{ox+Fe}}} - \frac{m_{\text{Fe}}^0}{\rho_{\text{Fe}} - \rho_{\text{ox+Fe}}} \quad (8)$$

$$V_{\text{Fe}} = \frac{\rho_{\text{ox+Fe}}}{\rho_{\text{ox+Fe}} - \rho_{\text{Fe}}} V_{\text{total}} - \frac{m_{\text{ox}}^0}{\rho_{\text{ox+Fe}} - \rho_{\text{Fe}}} - \frac{m_{\text{Fe}}^0}{\rho_{\text{ox+Fe}} - \rho_{\text{Fe}}} \quad (9)$$

Figure 5 shows the results of the volume change of the compound droplet composed of Fe and Flux-9 ($V_{\text{total}} = V_{\text{Fe}} + V_{\text{shell}}$). In the same figure, the core Fe volume determined from X-ray radiographic images before and after melting, as well as the oxide shell volume estimated by subtracting the core volume from the total volume, are plotted as data points. Additionally, estimated volume change of V_{Fe} and V_{shell} are shown for four assumed Fe mass dissolution ratios into the oxide: 0.125, 0.25, 0.375, 0.5, for a sample held at 1610 °C for 1.2×10^3 s. The results indicate that a higher Fe dissolution ratio into the oxide corresponds to a greater deviation from the initial volume. The shell volume, V_{shell} , increases using the density of Flux-9 with adding Fe and correlates well with the shell volume, V_{shell} . Therefore, the volume expansion of the core-shell droplets is concluded by the Fe dissolution from the core Fe to the shell oxide during the melting experiments in ELF. The Fe dissolution into the shell oxide is larger than the thermal equilibrium. The Fe dissolution for this density increase is due to liquid Fe oxidation. Since the sample's mass did not change before and after melting, it is unlikely that the oxygen used for oxidation was supplied from the outside. The oxygen used source for the liquid Fe oxidation at the interface is attributed to the oxygen included in the core Fe¹⁷) and/or the oxygen from the reaction in the molten oxide where Fe_2O_3 decomposed to Fe_3O_4 and O_2 ($6\text{Fe}_2\text{O}_3 \rightarrow 4\text{Fe}_3\text{O}_4 + \text{O}_2$).¹⁹) Decomposed oxygen from Fe_2O_3 near the interface is absorbed on the liquid Fe and diffused as FeO into the shell oxide, decomposing into Fe and O. The Fe decomposed from FeO diffused into the shell, oxide expands in volume because the Fe in the oxide breaks the oxide network structure. Moreover, we should consider the effect of an electrical double layer¹⁹) at the interface between liquid Fe and molten oxide because the core-shell droplet stays in the electrical charge at the interface would affect the change in interfacial properties. The emulsification phenomenon of liquid Fe in oxide melts containing FeO was recently observed using X-ray Computed Tomograph method.^{20–22}) The results suggest that oxygen movement at the interface between liquid Fe and FeO-containing oxide melts triggers the emulsification phenomenon.²¹) X-ray transmitted images of Fe/Flux-9 compound droplets, as shown in **Fig.2**, also revealed Fe particles dispersed within the shell oxide. However, in this case, the increase in the volume of molten oxide with $\text{SiO}_2\text{:CaO:Mn}_3\text{O}_4\text{:TiO}_2\text{:Fe}_2\text{O}_3 = 25\text{:}7\text{:}20\text{:}18\text{:}30$ mass% compositions do not contribute to the phenomenon. Therefore, further investigation is necessary to determine the extent of core Fe reduction caused by the emulsification phenomenon.

This phenomenon of dissolution and diffusion of Fe from liquid Fe into the oxide and the increase in the volume of the molten oxide are challenging to observe on the ground, and we believe that it was first observed in the levitation experiment in a microgravity environment. In the future, we will elucidate the oxygen source causing the liquid Fe oxidation and explore the behavior of liquid Fe and molten oxide at the core-shell droplet interface.

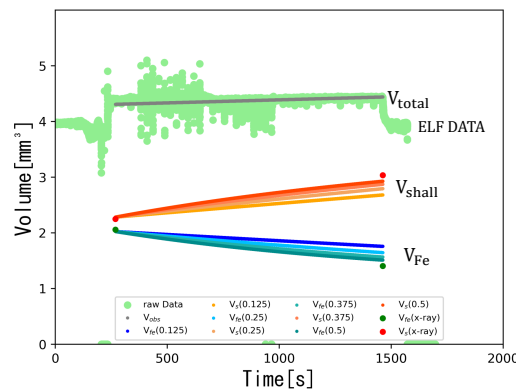


Figure 5. The estimated volumes of the compound droplet composed of Fe and Flux-9 (V_{total}), the shell oxide with dissolved Fe (V_{shell}), and the liquid core Fe (V_{Fe}) are shown, along with the experimentally measured volume of the compound droplet using the ELF under microgravity.

Conclusion

Core-shell droplets composed of liquid Fe and molten oxide were produced using the ELF on board the ISS, and their volume change was observed at 1610 °C. The droplet volume increased over approximately 20 minutes, which is attributed to the oxidation of liquid Fe and its subsequent dissolution into the shell oxide. The dissolved Fe likely disrupted the oxide structure, resulting to expansion. This phenomenon was clearly observed under microgravity, and future investigation is needed to elucidate the interfacial phenomena in detail.

Acknowledgements

We thank Prof. Takehiko Ishikawa and Mr. Yuki Watanabe of Japan Aerospace Exploration Agency for their support of onboard experiments and valuable discussions on ISS-ELF experimental details. We also thank Japan Manned Space Co. Ltd. (JAMSS) for supporting this research.

Conflicts of Interest

The authors state no conflict of interest.

References

- 1) K. Ogino: Interfacial Tension Between Molten Iron Alloys and Molten Slags (in Japanese), *Tetsu-to-Hagane*, 61 (1975) 2118.
- 2) T. Matsushita and T. Watanabe: Dynamic In Situ X-ray Observation of a Molten Steel Drop Shape Change in Molten Slag, *Miner. Process. Extr. Metall.*, 120 (2011) 49.
- 3) H. Tamaru, T. Ishikawa, J. T. Okada, Y. Nakamura, H. Ohkuma, S. Yukizono, Y. Sakai and T. Takada: Overview of the Electrostatic Levitation Furnace (ELF) for the International Space Station (ISS), *Int. J. Microgravity Sci. Appl.*, 32 (2015) 32104 (in Japanese).
- 4) T. Ishikawa, J. T. Okada, Y. Watanabe, H. Tamaru, Y. Nakamura: Thermophysical Property Measurements of Oxide Melts at High Temperature by Electrostatic Levitation Furnace on the ISS, *Int. J. Microgravity Sci. Appl.*, 32 (2015) 32041.
- 5) T. Ishikawa, C. Koyama, H. Tamaru, H. Saruwatari, M. Ohshio, Y. Nakamura: Status of the Electrostatic Levitation Furnace in the ISS— Evaluation of Sample Position Control, *Int. J. Microgravity Sci. Appl.*, 35 (2018) 350205.
- 6) T. Ishikawa, C. Koyama, H. Oda, H. Sarukura, P.-F. Paradis: Status of the Electrostatic Levitation Furnace in the ISS— Surface Tension and Viscosity Measurements, *Int. J. Microgravity Sci. Appl.*, 39 (2022) 390101.
- 7) I. Matsumoto, R. Sato, M. Watanabe and T. Matsushita: Volume change of core-shell droplets of liquid iron and molten oxide under microgravity conditions, *High Temperatures-High Pressures*, 54 (2025) 101–111.
- 8) S. Taguchi, H. Hasome, S. Shimizu, R. Ishiwata, R. Inoue, M. Yamada, M. Watanabe, T. Matsushita, T. Ishikawa, H. Oda, C. Koyama and T. Ito: Proposal of Temperature Correction of Molten Oxide Based on Its Emissivity for Measurement of Temperature Dependence of Its Density Using ELF in ISS, *Int. J. Microgravity Sci. Appl.*, 40 (2023) 400101.
- 9) R. Sato, R. Ishiwata, S. Taguchi, and M. Watanabe: Measurement of the Normal Spectral Emissivity of Molten Oxide Using an Electromagnetically Levitated Complex Droplet of Molten Oxide and Liquid Fe, *High Temperature-High Pressure*, 52 (2023) 249–262.
- 10) S. Watanabe, Y. Tsu, K. Takano and Y. Shiraishi: Density of Pure Iron in Solid and Liquid States (in Japanese), *J. Jpn. Inst. Met.*, 45 (1981) 242.
- 11) J. Brillo and I. Egry: Density and excess volume of liquid copper, nickel, iron, and their binary alloys, *Int. J. Mat. Res.*, 95 (2022) 691.
- 12) A. Nakamura, S. Hakamada, A. Mizuno and M. Watanabe: Density Measurement of Molten Oxides of SiO₂-CaO-Al₂O₃ System by Aerodynamic Levitated Technique, *Int. J. Microgravity Sci. Appl.*, 34 (2017) 340404.
- 13) M. Watanabe, S. Ozawa, H. Fukuyama, T. Tsukada, and T. Hibiya: Levitation Research in Japan, in H.-J. Fecht, and M. Mohr (eds), *Metallurgy in Space, The Minerals, Metals & Materials Series*. (Springer, Cham.).
- 14) M. Watanabe, M. Adachi and H. Fukuyama: Densities of Fe–Ni melts and thermodynamic correlations, *J. Mat. Sci.*, 51 (2016) 3303.
- 15) M. J. Assael and K. Kakosimos, R. M. Banish, J. Brillo, I. Egry, R. Brooks, P. N. Quested, and K. C. Mills, A. Nagashima, Y. Sato W. A. Wakeham: Reference Data for the Density and Viscosity of Liquid Aluminum and Liquid Iron, *J. Phys. Chem. Ref. Data* 35 (2006) 285.
- 16) Thermo-Calc Software AB: TCOX12 Technical Information, Thermo-Calc Software (2017).
- 17) K. Ogino, S. Hara, T. Miwa and S. Kimoto: The Effect of Oxygen Content in Molten Steel on the Interfacial Tension Between Molten Steel and Slag (in Japanese), *Tetsu-to-Hagane*, 65 (1979) 2012.
- 18) J. Wiencke, H. Lavelaine, P.-J. Panteix, C. Petitjean and C. Rapin: Electrolysis of Iron in a Molten Oxide Electrolyte, *J. Appl. Electrochem.*, 48 (2018) 115.
- 19) E. Karimi-Sibaki, A. Kharicha, M. Wu, A. Ludwig and J. Bohacek: Modeling Electrochemical Transport of Ions in the Molten CaF₂-FeO Slag Operating Under a DC Voltage, *Appl. Math. Comput.*
- 20) M. A. Rhamdhani, K. S. Coley and G. A. Brooks: Kinetics of metal/slag reactions during spontaneous emulsification, *Metall Mater Trans, B36* (2005) 219–227.

- 21) S. Spooner, A. N. Assis, J. Warnett, J. et al.: Investigation into the Cause of Spontaneous Emulsification of a Free Steel Droplet; Validation of the Chemical Exchange Pathway, Metall Mater Trans, B 47(2016) 2123–2132.
- 22) S. Spooner, Z. Li, S. Sridhar: Spontaneous Emulsification as a Function of Material Exchange, Sci. Rep., 7(2017)5450.



© 2025 by the authors. This article is an open access article distributed under the terms and conditions of the Creative Commons Attribution (CC BY) license (<https://creativecommons.org/licenses/by/4.0/>).